**Supplementary Information**

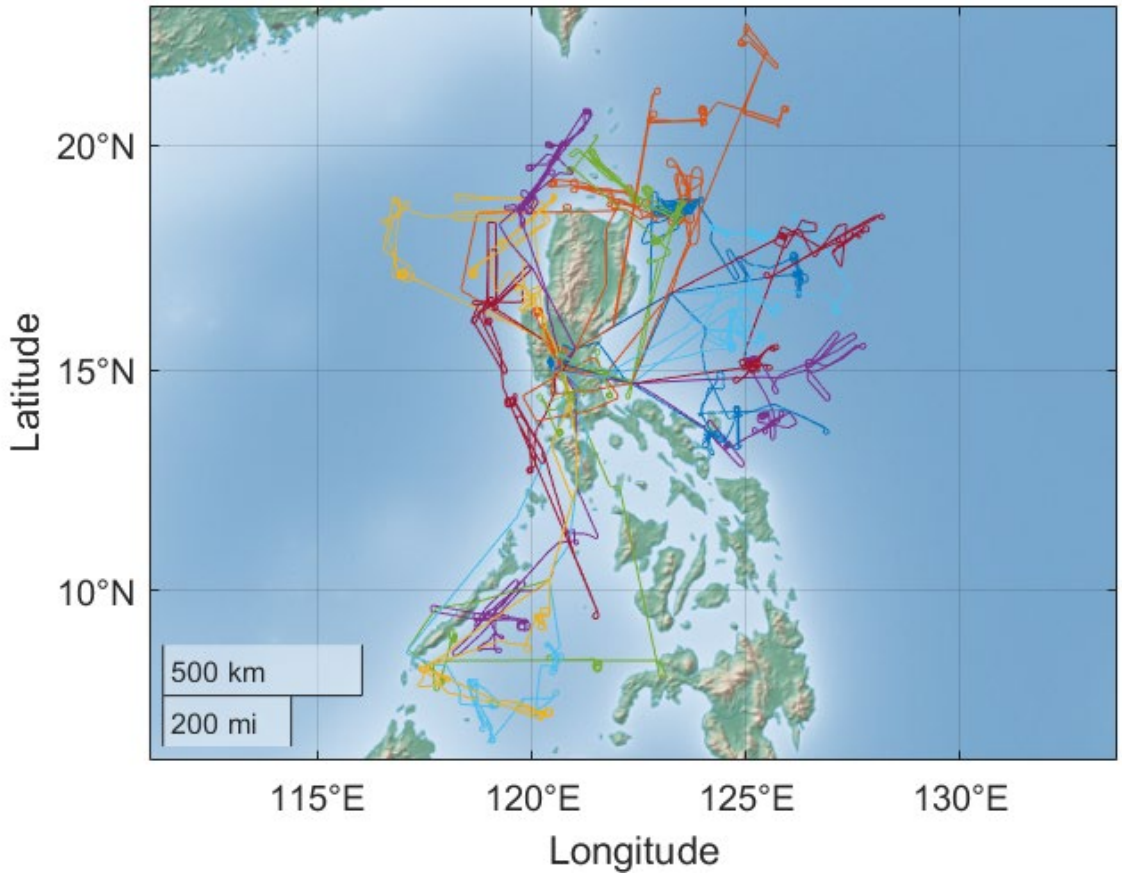


**Figure S1. Flight tracks of 19 RFs (24 August 2019 to 5 October 2019) during the CAMP2Ex field campaign.**

**Estimation of UV Actinic Flux from Irradiance**

To evaluate the actinic flux during NPF events observed in the early morning (see Sect. 4.1), we estimated UV actinic flux from irradiance measurements, solar zenith angle (SZA), and sky condition (Kylling et al., 2003; Webb et al., 2002). When SZA is higher than 60º or under clear sky conditions, the downwelling irradiance is assumed as direct only (Kylling et al., 2003), and total actinic flux is given by:

$$E_{UV} = \frac{F_{dn}}{\cos(SZA)} + 2 \cdot F_{up} \qquad (S1)$$

Where $E_{UV}$ represents actinic flux over the UV wavelength range, $F_{dn}$ and $F_{up}$ are the downwelling and upwelling components of UV irradiance. Under cloudy and overcast conditions, actinic flux is simply twice the sum of both components (Kylling et al., 2003). We utilized the zenith cloud mask data to help identify the cloud conditions, which is developed using Cloud Detection Neural Network (CDNN; Nied et al., submitted) based on forward camera onboard the aircraft. The UV irradiance and estimated actinic flux during the early morning NPF events (7:00-10:00, local time) are compared with those during NPF events observed around noon time (10:00-14:00, Fig. S2).

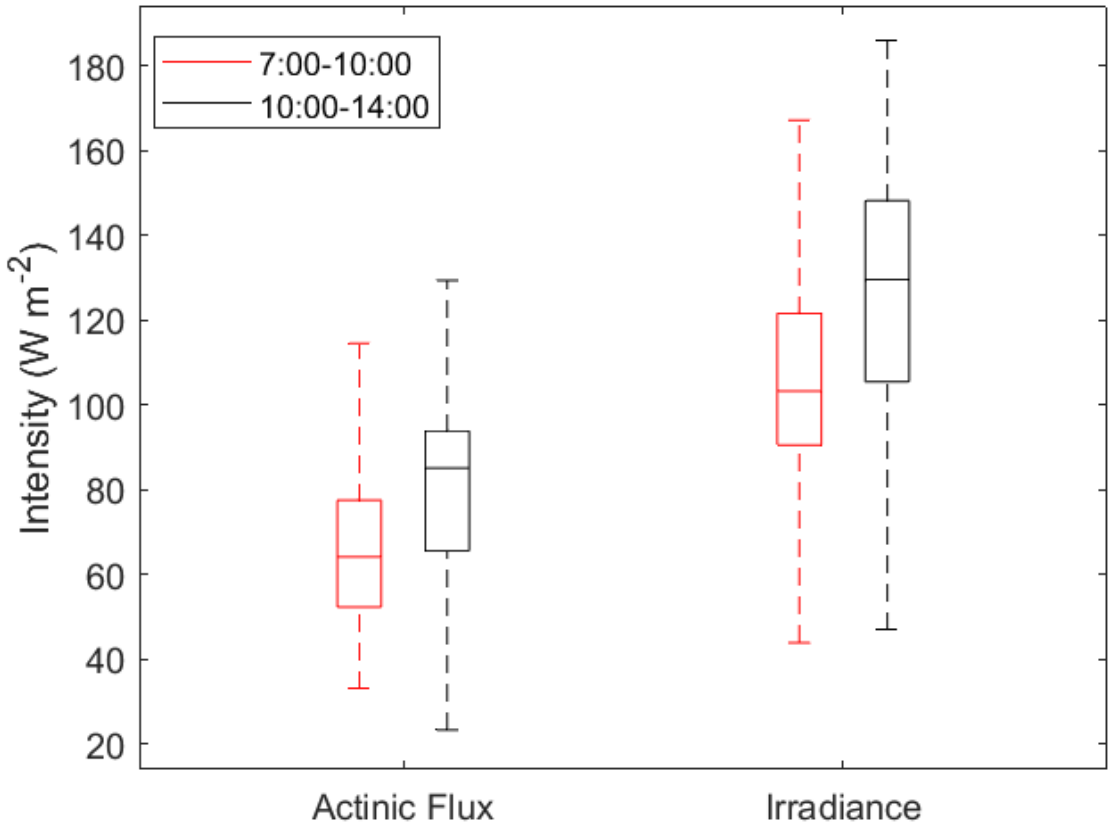

**Figure S2. Statistical comparison of UV irradiance and estimated actinic flux during the early morning background NPF events (7:00-10:00, red) and those during NPF events observed around noon time in the same altitude range (6.5-7.2 km, black).**

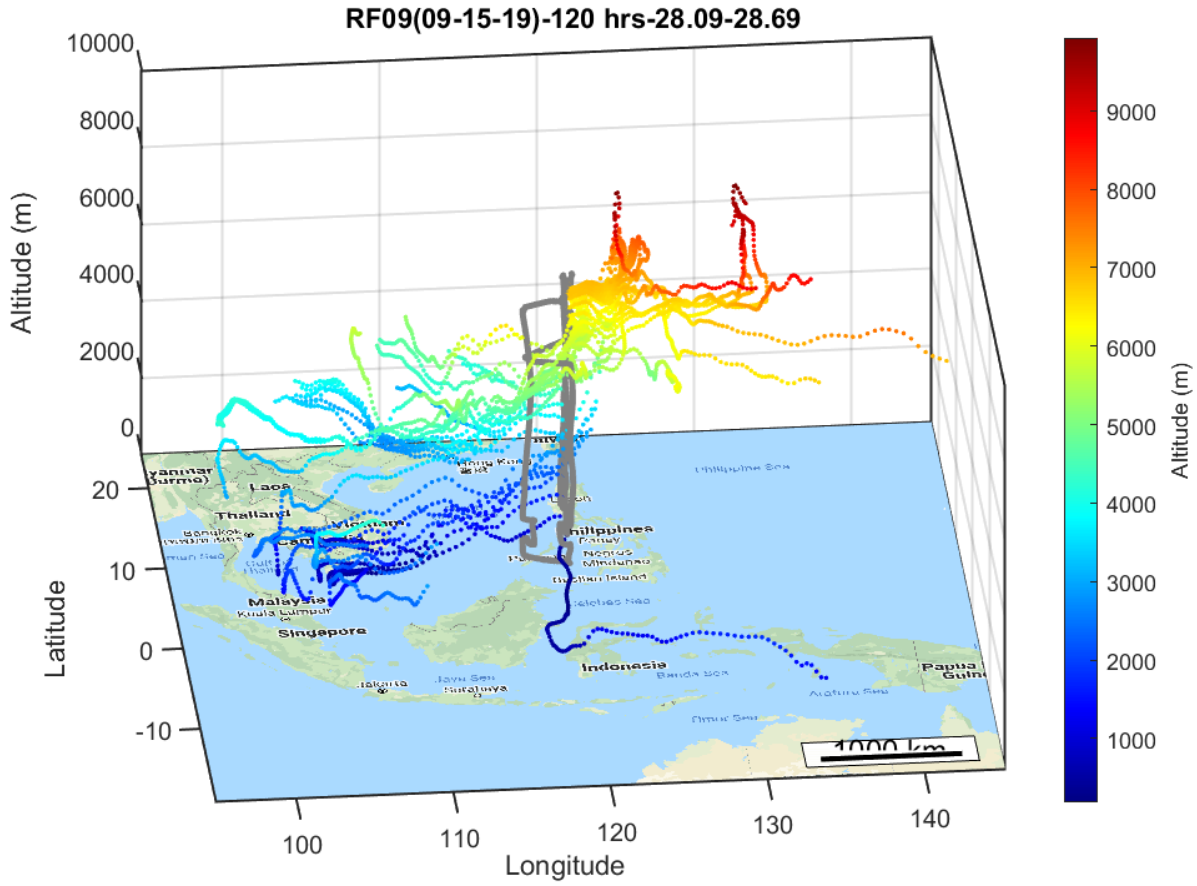


**Figure S3. 3-D plot of 120-hour backward trajectories for air masses arriving at the locations where NPF was observed at 6.7 km and along an ascending flight segment, color coded by altitude (meter above sea level). Each trajectory was calculated every 1 min.**

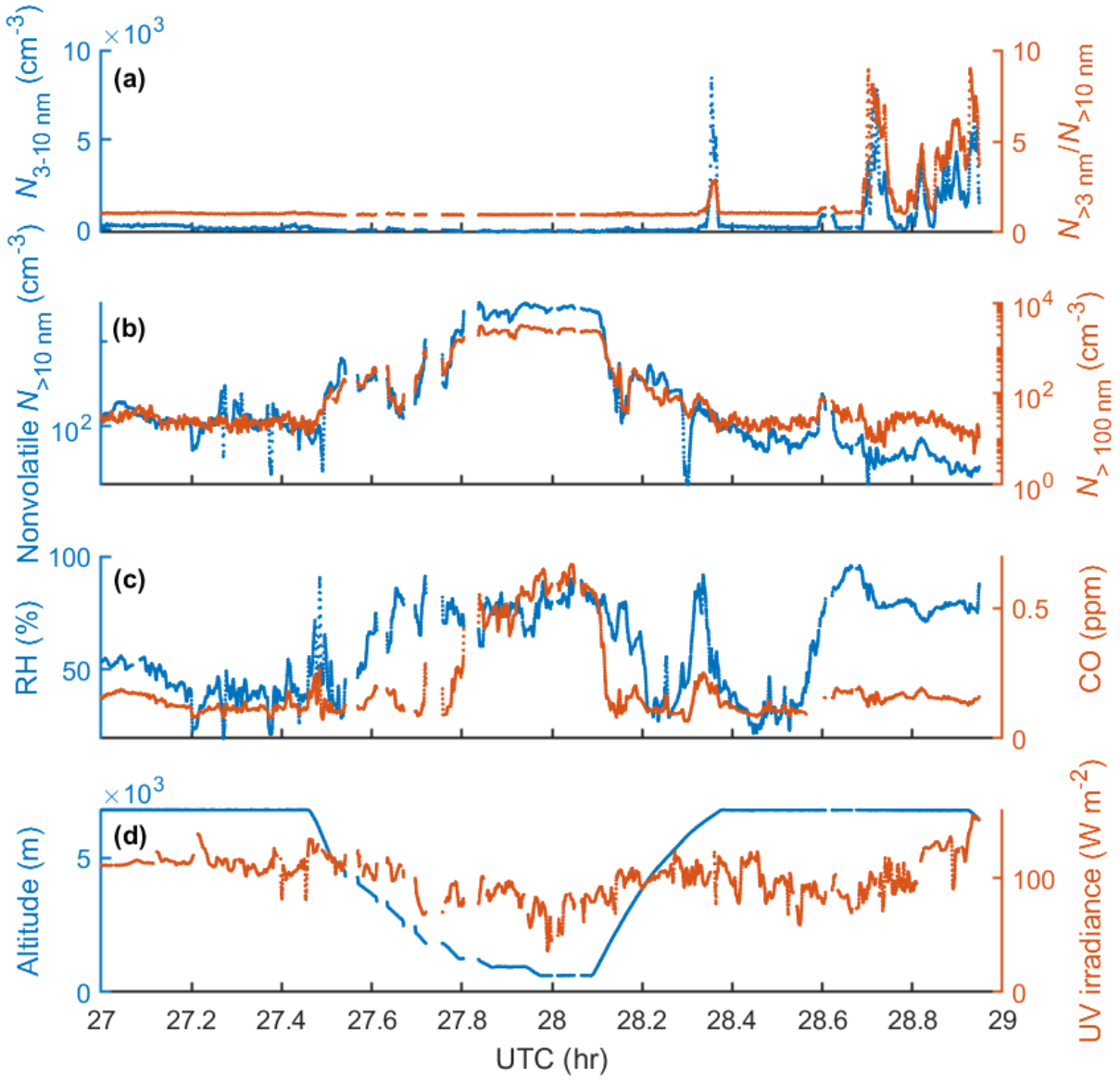


**Figure S4. Time series of selected periods during RF9 (15 September 2019). There were two level flight segments at 6.7 km, one of which (UTC 27-27.5) did not coincide with NPF while NPF was observed during the other (UTC 28.4-28.9).**

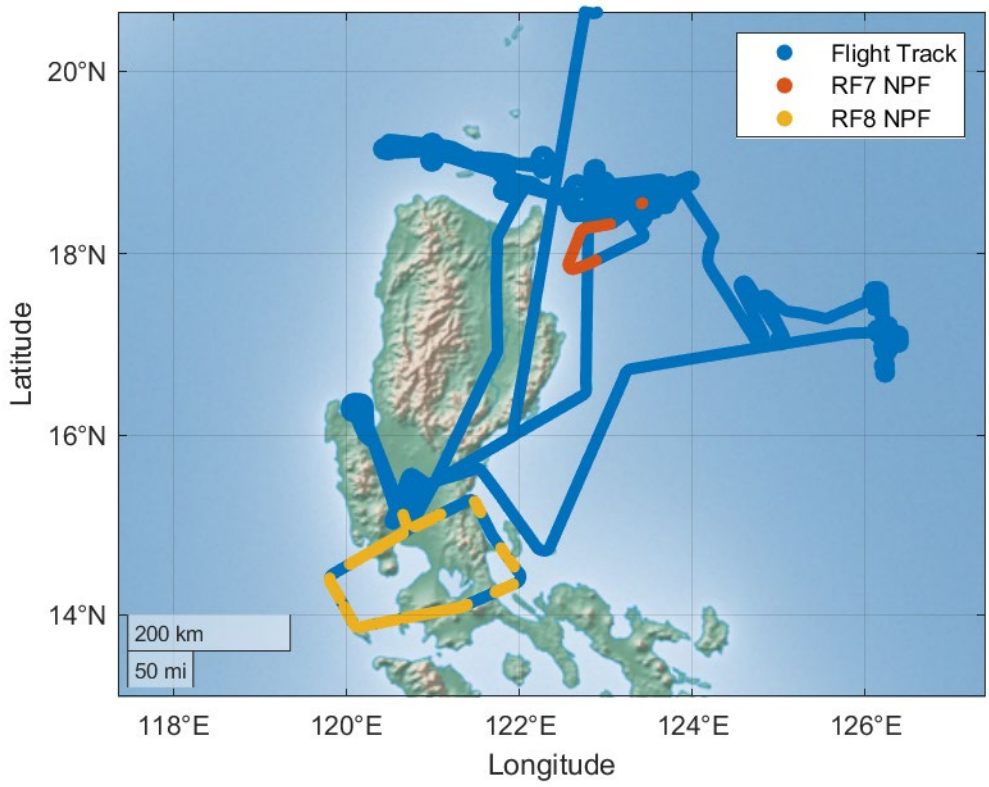


**Figure S5. Flight tracks of RF7 (8 September 2019, East of Luzon) and RF8 (13 September 2019, loop around Luzon and Metro Manila). Red segments represent the NPF events classified as urban influenced (included in cluster #3), and yellow represents NPF during RF8.**

**Table S1. Overview of P-3B research flights (RFs) performed during the campaign. The values of altitude, RH and CPC data are presented as mean value ± standard deviation (σ). Altitude data are reported in meters above sea level.**

| Date | RF No. | Location | NPF Duration, s | Altitude, m | RH, % | $N_{>3\ nm}/N_{>10\ nm}$ | $N_{3\text{-}10\ nm}$ |
|---|---|---|---|---|---|---|---|
| 08/24/2019 | 1 | Loop around Luzon | 108 | 6090±1598 | 45.9±19.3 | 1.43±0.12 | 493±240 |
| 08/27/2019 | 2 | NW Luzon | 2140 | 7119 ±323 | 71.5±18.7 | 2.10±0.51 | 1223±762 |
| 08/29/2019 | 3 | Sulu Sea | 1340 | 7642±308 | N/A | 2.57±1.79 | 2671±2897 |
| 08/30/2019 | 4 | Palawan/ Sulu Sea | 5130 | 7155±1108 | 80.6±10.2 | 2.19±1.28 | 2985±3989 |
| 09/04/2019 | 5 | Palawan/ Sulu Sea | 360 | 7630±234 | 73.3±4.5 | 2.11±0.73 | 1435±1311 |
| 09/06/2019 | 6 | West Luzon/ Sulu Sea | 900 | 7448±3 | 86.2±4.7 | 1.66±2.73 | 1252±708 |
| 09/08/2019 | 7 | East Luzon | 2730 | 6711±758 | 62.2±19.5 | 3.86±6.01 | 842±724 |
| 09/13/2019 | 8 | Loop around Luzon | 2200 | 5750±261 | 78.1±8.8 | 2.23±1.44 | 2091±3366 |
| 09/15/2019 | 9 | Palawan/ Sulu Sea | 880 | 6741±88 | 76.1±8.0 | 4.27±2.05 | 2607±1901 |
| 09/16/2019 | 10 | East Luzon | 840 | 6864±497 | 68.2±11.1 | 2.41±1.87 | 1778±3081 |
| 09/19/2019 | 11 | North Luzon | 80 | 6752±2 | 28.5±1.1 | 2.25±1.22 | 1537±1537 |
| 09/21/2019 | 12 | North/East Luzon | N/A | N/A | N/A | N/A | N/A |
| 09/23/2019 | 13 | East Luzon | N/A | N/A | N/A | N/A | N/A |
| 09/25/2019 | 14 | East Luzon | N/A | N/A | N/A | N/A | N/A |
| 09/27/2019 | 15 | East Luzon | N/A | N/A | N/A | N/A | N/A |
| 09/29/2019 | 16 | West Luzon | N/A | N/A | N/A | N/A | N/A |
| 10/01/3019 | 17 | West Luzon | N/A | N/A | N/A | N/A | N/A |
| 10/03/2019 | 18 | Manila | 170 | 4827±2 | 77.8±2.5 | 2.13±0.47 | 2288±1409 |
| 10/05/2019 | 19 | East Luzon | 690 | 6579±930 | 59.3±5.8 | 1.65±0.46 | 3321±3212 |

**References**

Kylling, A., Webb, A. R., Bais, A. F., Blumthaler, M., Schmitt, R., Thiel, S., Kazantzidis, A., Kift, R., Misslbeck, M., Schallhart, B., Schreder, J., Topaloglou, C., Kazadzis, S., and Rimmer, J.: Actinic flux determination from measurements of irradiance, Journal of Geophysical Research: Atmospheres, 108, https://doi.org/10.1029/2002JD003236, 2003.

Webb, A. R., Bais, A. F., Blumthaler, M., Gobbi, G.-P., Kylling, A., Schmitt, R., Thiel, S., Barnaba, F., Danielsen, T., Junkermann, W., Kazantzidis, A., Kelly, P., Kift, R., Liberti, G. L., Misslbeck, M., Schallhart, B., Schreder, J., and Topaloglou, C.: Measuring Spectral Actinic Flux and Irradiance: Experimental Results from the Actinic Flux Determination from Measurements of Irradiance (ADMIRA) Project, Journal of Atmospheric and Oceanic Technology, 19, 1049-1062, 10.1175/1520-0426(2002)019<1049:Msafai>2.0.Co;2, 2002.

Nied, J., Jones, M., Seaman, S., Shingler, T., Hair, J., Cairns, B., Van Gilst, D., Bucholtz, A., Schmidt, S., Chellappan, S., Zuidema, P., Van Diedenhoven, B., Sorooshian, A., and Stamnes, S.. "A cloud detection neural network for above-aircraft clouds using airborne cameras." *Frontiers in Remote Sensing* (submitted).